Molecular Biology of the Cell
Vol. 18, 1781–1789, May 2007

Direct Binding to Rsp5p Regulates Ubiquitination-independent Vacuolar Transport of Sna3p

Hadiya Watson and Juan S. Bonifacino

Cell Biology and Metabolism Branch, National Institute of Child Health and Human Development, National Institutes of Health, Bethesda, MD 20892

Submitted October 4, 2006; Revised January 19, 2007; Accepted February 20, 2007
Monitoring Editor: Jean Gruenberg

The sorting of integral membrane proteins such as carboxypeptidase S (Cps1p) into the luminal vesicles of multivesicular bodies (MVBs) in *Saccharomyces cerevisiae* requires ubiquitination of their cytosolic domains by the ubiquitin ligases Rsp5p and/or Tul1p. An exception is Sna3p, which does not require ubiquitination for entry into MVBs. The mechanism underlying this ubiquitination-independent MVB sorting pathway has not yet been characterized. Here, we show that Sna3p sorting into the MVB pathway depends on a direct interaction between a PPAY motif within its C-terminal cytosolic tail and the WW domains of Rsp5p. Disruption of this interaction inhibits vacuolar targeting of Sna3p and causes its accumulation in a compartment that overlaps only partially with MVBs. Surprisingly, Sna3p does require a functional ubiquitin-ligase HECT domain within Rsp5p; however, the dependence of Sna3p on HECT domain activity is distinct from that of Cps1p. Last, we show that Sna3p requires neither Tul1p nor the transmembrane adaptor protein Bsd2p for its MVB sorting. Our data demonstrate that Sna3p follows a novel ubiquitination-independent, but Rsp5p-mediated, sorting pathway to the vacuole.

INTRODUCTION

The delivery of most endocytic and biosynthetic cargo proteins to the *Saccharomyces cerevisiae* vacuole requires their prior transit through one or more classes of endosomes. Multivesicular bodies (MVBs) are a discrete class of late endosomal compartments that contain intraluminal vesicles formed by invagination of the endosomal limiting membrane (Odorizzi *et al*., 1998; Katzmann *et al*., 2002). On fusion of MVBs with the vacuole, these intraluminal vesicles are delivered to the lytic environment of the vacuolar lumen for degradation.

Formation of and exit from MVBs are regulated by "class E" vacuolar protein sorting (Vps) proteins, the loss of which results in the accumulation of both biosynthetic and endocytic cargo into an exaggerated late endosomal structure termed the "class E compartment" (Rieder *et al*., 1996; Odorizzi *et al*., 1998). Recent studies have shown that biosynthetic integral membrane protein cargo such as carboxypeptidase S (Cps1p) and the polyphosphatase Phm5p are marked for delivery into the intraluminal vesicles of MVBs by monoubiquitination of their cytosolic domains (Katzmann *et al*., 2001; Reggiori and Pelham, 2001; Urbanowski and Piper, 2001; for review, see Hicke and Dunn, 2003). Recognition and sorting of monoubiquitinated MVB cargo is carried out by a subset of class E Vps proteins that assemble into several *e*ndosomal *s*orting *c*omplexes *r*equired for *t*ransport (ESCRTs) (for review, see Hurley and Emr, 2006). Loss of cargo ubiquitination via mutations of the cytosolic Lys residues within such proteins precludes their entry into MVBs and results in their accumulation on the limiting membrane of the vacuole (Katzmann *et al*., 2001).

This article was published online ahead of print in *MBC in Press* (http://www.molbiolcell.org/cgi/doi/10.1091/mbc.E06–10–0887) on March 1, 2007.

Address correspondence to: Juan S. Bonifacino (juan@helix.nih.gov).

The HECT-domain E3 ubiquitin ligase Rsp5p has recently been implicated in the ubiquitination of Cps1p and Phm5p (Reggiori and Pelham, 2001; Hettema *et al*., 2004; Katzmann *et al*., 2004), in addition to its role in the ubiquitination and internalization of various endocytic cargo proteins (Dunn and Hicke, 2001b). Rsp5p-catalyzed MVB cargo ubiquitination is mediated by an interaction between a PPTY motif within the transmembrane adaptor protein Bsd2p and the WW domains of Rsp5p (Hettema *et al*., 2004). A study by Katzmann *et al*. (2004) identified an allele of *RSP5* (mvb326; G555D) that is specifically defective for modifying Cps1p. However, this study also demonstrated that other previously characterized mutant *rsp5* alleles that are deficient in endocytic cargo ubiquitination (e.g., rsp5-1; L733S) do not affect Cps1p MVB sorting.

Sna3p is another integral membrane protein that follows the MVB pathway into the vacuolar lumen (Reggiori and Pelham, 2001). Like other cargo, MVB sorting of Sna3p depends on functional class E Vps proteins; however, Sna3p is the only transmembrane cargo identified thus far in yeast that does not require ubiquitination of its cytosolic Lys residues to enter MVBs (Reggiori and Pelham, 2001). Furthermore, Bilodeau *et al*. (2002) have shown that the ubiquitin-interacting motifs within two key ESCRT complex-associated proteins (Vps27p and Hse1p) are also not required for Sna3p sorting. Since these initial findings, the mechanism underlying this ubiquitination-independent MVB sorting pathway has not been characterized.

In this study, we show that Sna3p sorting into the MVB pathway is, paradoxically, mediated by a direct interaction between a PPAY motif within its C-terminal cytosolic domain and the WW domains of Rsp5p. Mutation of the PPAY motif not only inhibits vacuolar targeting of Sna3p but also causes its accumulation in an aberrant compartment that may lie upstream of the MVB. Similarly, Sna3p sorting is disrupted in *rsp5* mutants lacking functional WW domains. Furthermore, although its direct ubiquitination is not required for sorting (Reggiori and Pelham, 2001), Sna3p nonetheless requires a

Table 1. Strain descriptions

Strain	Genotype	Source
BY4742	MATα *his3*Δ*1 leu2*Δ*0 lys2*Δ*0 ura3*Δ*0*	Research Genetics (Huntsville, AL)
sna3Δ	MATα *his3*Δ*1 leu2*Δ*0 lys2*Δ*0 ura3*Δ*0 sna3*Δ*::Kan*	Research Genetics
vps27Δ	MATα *his3*Δ*1 leu2*Δ*0 lys2*Δ*0 ura3*Δ*0 vps27*Δ*::Kan*	Research Genetics
pep12Δ	MATα *his3*Δ*1 leu2*Δ*0 lys2*Δ*0 ura3*Δ*0 pep12*Δ*::Kan*	Research Genetics
end3Δ	MATα *his3*Δ*1 leu2*Δ*0 lys2*Δ*0 ura3*Δ*0 end3*Δ*::Kan*	Research Genetics
pep12Δ	MATα *his3*Δ*1 leu2*Δ*0 lys2*Δ*0 ura3*Δ*0 pep12*Δ*::Kan*	Research Genetics
tul1Δ	MATα *his3*Δ*1 leu2*Δ*0 lys2*Δ*0 ura3*Δ*0 tul1*Δ*::Kan*	Research Genetics
bsd2Δ	MATα *his3*Δ*1 leu2*Δ*0 lys2*Δ*0 ura3*Δ*0 bsd2*Δ*::Kan*	Research Genetics
HWY30	*MAT a rsp5*Δ*::HIS3 trp1 ura3 his3 leu2* YcpHA-*RSP5*	This study
HWY31	*MAT a rsp5*Δ*::HIS3 trp1 ura3 his3 leu2* pHW35	This study
HWY32	*MAT a rsp5*Δ*::HIS3 trp1 ura3 his3 leu2* pHW36	This study
HWY33	*MAT a rsp5*Δ*::HIS3 trp1 ura3 his3 leu2* pHW37	This study
LHY23	*MAT a 1 ura3 leu2 trp1 bar1 rsp5–1*	Stamenova *et al.* (2004)
LHY4366	*MAT a trp1 ura3 his3 leu2 rsp5*Δ*::HIS3* p*RSP5*[*TRP*]	Stamenova *et al.* (2004)

functional HECT domain within Rsp5p. Quite strikingly, the dependence of Sna3p on HECT domain ligase activity is distinct from that of Cps1p, because the sorting of Sna3p into the MVB pathway is unaffected in *rsp5*^{G555D} mutants, but completely disrupted in *rsp5-1* (L733S) mutants. Finally, we show that, unlike Cps1p, Sna3p does not require another E3 ubiquitin ligase, Tul1p, or the transmembrane adaptor protein Bsd2p for its MVB sorting. Together, our data show that Sna3p follows a novel ubiquitination-independent, but Rsp5p-mediated, sorting pathway to the vacuole.

MATERIALS AND METHODS

Media and Chemicals

S. cerevisiae strains were grown in standard yeast extract/peptone/dextrose (YPD) or synthetic medium with dextrose supplemented with the appropriate amino acids as required for plasmid maintenance. Bacterial strains were grown on standard media supplemented with 100 μg/ml ampicillin or 30 μg/ml kanamycin, as appropriate, to maintain plasmids. Chemicals were purchased from Fisher Scientific (Fairlawn, NJ) or Sigma-Aldrich (St. Louis, MO) unless stated otherwise.

Plasmid and Strain Construction

The strains and plasmids used in this study are listed in Tables 1 and 2, respectively. Strains LHY23 and LHY4366 were gifts from Linda Hicke (Northwestern University, Illinois). PHM5-GFP, YcpHA-RSP5, and DsRed-FYVE were gifts from Hugh Pelham (MRC Laboratory of Molecular Biology and Genetics, Germany), Teresa Zoladek (Polish Academy of Sciences, Poland), and Kai Simons (Max Planck Institute for Molecular Cell Biology and Genetics, Germany), respectively. DNA and strain manipulations were performed with the use of standard techniques. QuikChange polymerase chain reaction (PCR) (Stratagene, La Jolla, CA) was used for all mutagenesis unless otherwise stated.

Green Fluorescent Protein (GFP)-tagged Constructs. URA3-based GFP plasmids were constructed by inserting the following into pRS316: an ADH1 promoter within the KpnI/EcoRI sites, a GFP tag within the EcoRI/BamHI sites, and a CYC1 terminator within the XhoI/SacI sites to generate pCB1. LEU2-based GFP plasmids were constructed by inserting a KpnI–SacI fragment from pCB1-based plasmids into a pRS415 vector lacking the first KpnI site (position 1106). CPS1 was PCR-generated from genomic DNA and inserted into the BamHI/XhoI sites of pCB1 to create pHW1. Full-length SNA3 (base pairs 1-402) was generated by PCR by using a plasmid encoding Sna3p-GFP as a template (a gift from Hugh Pelham) and cloned as a BamHI–XhoI fragment into pCB1 to generate pHW18. To construct the SNA3 N-terminal truncation mutation, a PCR fragment consisting of base pairs 58-402 of SNA3 was inserted into the BamHI/XhoI sites of pCB1 to generate pHW19. SNA3 C-terminal truncations were constructed by inserting a stop codon at positions encoding amino acids 74, 109, 116, and 128 within pHW18. pHW18 was also used as a template to generate the Y109A mutation.

His$_6$- and GST-tagged Constructs. His$_6$-tagged constructs were created by inserting a PCR fragment consisting of base pairs 220–402 of SNA3 within the BamHI/SalI sites of pET28a (Novagen, San Diego, CA) to generate pHW27. This plasmid was used as a template to generate mutation Y109A. LHP703 was a gift from Linda Hicke.

Hemagglutinin (HA)-tagged RSP5 Constructs and Strains. YcpHA-RSP5 was used as a template to generate mutations G555D and L733S. WW domain mutations were generated within YcpHA-RSP5 by replacing tryptophan residues at positions 257, 359, and 415 with alanine. The aforementioned plasmids were then transformed into LHY4366 and transformants were grown on medium containing 5-fluoroanthranilic acid to remove the TRP-based plasmid. Expression of the proteins was confirmed by immunoblotting with monoclonal antibody (mAb) to the HA epitope.

N-(3-Triethylammoniumpropyl)-4-(p-diethylaminophenylhexatrienyl) Pyridinium Dibromide (FM4-64) Labeling

Cells were grown to mid-log phase in selective medium at 30°C, harvested at 2000 rpm, and labeled with 80 μM FM4-64 in YPD for 20 min. After two

Table 2. Plasmid descriptions

Plasmid	Description	Source
pCB1[a]	ADH1/GFP/CYC1 pRS316	This study
pHW1	GFP-CPS^{WT}	This study
pHW18	GFP-SNA3^{WT}	This study
pHW19	GFP-SNA3$^{\Delta 1\text{-}18}$	This study
pHW20	GFP-SNA3$^{\Delta 128\text{-}133}$	This study
pHW21	GFP-SNA3$^{\Delta 109\text{-}133}$	This study
pHW22	GFP-SNA3$^{\Delta 116\text{-}133}$	This study
pHW23	GFP-SNA3$^{\Delta 74\text{-}133}$	This study
pHH1[b]	ADH1/GFP/CYC1 pRS415	This study
pHH2	GFP-CPS^{WT}	This study
pHW25	GFP-SNA3^{WT}	This study
pHW27	His$_6$-SNA3 Cterm	This study
pHW28	His$_6$-SNA3 Cterm^{Y109A}	This study
pHW35	HA-RSP5$^{ww1\text{-}3\ mut}$	This study
pHW36	HA-RSP5^{G555D}	This study
pHW37	HA-RSP5^{L733S}	This study
LHP703	GST-RSP5$^{WW1\text{-}3}$	Stamenova *et al.* (2004)
pHW38	GST-RSP5 FL^{WT}	Gift from Claudio Aguilar
PHW39	GST-RSP5 FL$^{ww1\text{-}3\ mut}$	This study
YcpHA-RSP5	HA-RSP5	Kaminka *et al.* (2002)
Phm5-GFP	Phm5-GFP	Reggiori and Pelham (2001)

[a] Plasmids pHW1 and pHW18-pHW23 were expressed in pCB1.
[b] Plasmids pHH2 and pHW25 were expressed in pHH1.

washes, cells were chased with YPD for 40 min at 30°C. Cells were viewed with a 100× objective lens on an IX-70 fluorescence microscope (Olympus, Tokyo, Japan; excitation, 560 nm; dichroic mirror at 595 nm; and emission, 630 nm). Images were captured digitally with an IMAGO charge-coupled device camera controlled by TILLvisION software (TILL Photonics, Eugene, OR). Images were processed using Adobe Photoshop 5.0 (Adobe Systems, Mountain View, CA).

Preparation of Cell Lysates for Immunoblotting

For detection of GFP-tagged proteins, 5 OD_{600} of cells was harvested, and whole cell extracts were prepared by glass bead lysis in Laemmli's sample buffer. Samples were analyzed by SDS-polyacrylamide gel electrophoresis (PAGE) and immunoblotting with a mAb to GFP (Roche Diagnostics, Indianapolis, IN).

Metabolic Labeling and Immunoprecipitation

Metabolic labeling of yeast cells with ^{35}S Express label (PerkinElmer Life and Analytical Sciences, Boston, MA), pulse-chase analyses, and immunoprecipitations were performed at 30°C as described by Bonangelino *et al*. (2002). Briefly, a 10-min pulse, followed by a 40-min chase, was used. Immunoprecipitations were performed overnight at 4°C, and the immunoprecipitates were analyzed by SDS-PAGE and autoradiography. A polyclonal antibody to Cps1p was a gift from Greg Payne (UCLA, California).

Coimmunoprecipitation

Twenty OD_{600} of cells grown to mid-log phase were lysed in TBS-T (Tris-buffered saline/Tween 20; 10 mM Tris, 140 mM NaCl, and 0.1% Tween 20, pH 7.5) supplemented with protease inhibitor cocktail (Roche Diagnostics) by using the glass bead lysis method. Lysates were centrifuged for 10 min at 14,000 rpm at 4°C, and supernatants were precleared by incubation for 60 min at 4°C with 30 μl of protein A-Sepharose beads (GE Healthcare, Little Chalfont, Buckinghamshire, United Kingdom) and centrifugation at 8000 × *g* for 5 min. The precleared lysates were subsequently incubated for 2 h at 4°C with 30 μl of protein A-Sepharose beads bound to rabbit polyclonal antibody to the HA epitope (Covance, Princeton, NJ). After immunoprecipitation, the beads were washed four times with TBS-T. Washed beads were subjected to SDS-PAGE and immunoblotting analysis with either mouse monoclonal anti-HA or mouse monoclonal anti-GFP (Roche Diagnostics).

Recombinant His_6-tagged and GST Fusion Protein Expression and Purification

Protein expression was induced in *Rosetta* cells (Novagen) transformed with pET28a- or pGEX-derived constructs by the addition of isopropyl-β-D-thiogalactopyranoside (1 mM final concentration) followed by a 3-h incubation at 37°C. The cells were harvested, resuspended in TBS-T, pH 8.0, and sonicated. Lysates were centrifuged for 30 min at 15,000 rpm at 4°C in a centrifuge (Sorvall, Newton, CT), and the supernatants were collected. For glutathione *S*-transferase (GST) fusion protein purification, the lysates were incubated in batch with agarose beads coupled to glutathione for 2 h at 4°C and then washed four times with TBST.

GST Pull-Down Assays

Glutathione-agarose beads (Sigma-Aldrich) loaded with either GST or GST fusion proteins were incubated with bacterial lysates containing His_6-tagged recombinant protein for 1 h at 4°C. Samples were centrifuged at 1000 rpm, unbound material was collected, and beads were washed three times with TBS-T. Samples were boiled in Laemmli's sample buffer and resolved by SDS-PAGE followed by immunoblotting by using either rabbit anti-GST (Invitrogen, Carlsbad, CA) or mouse anti-His_6 (Novagen).

RESULTS

Targeting of Sna3p to the Vacuole Is Mediated by Its C-Terminal Tail

Sna3p is a small (133-amino acid) integral membrane protein that contains two transmembrane domains connected by a short luminal loop, and two cytosolic tails at its N and C termini (Figure 1, A and B). Sna3p contains only two cytoplasmic Lys residues (black circles): one at the N terminus (K19) and the other at the C terminus (K125). Mutation of both residues was previously found not to affect vacuolar targeting of Sna3p tagged with GFP at either its C terminus (Reggiori and Pelham, 2001) or its N terminus (our unpublished data). To determine what region of Sna3p is required for its vacuolar targeting, GFP was fused to the N terminus of Sna3p (Figure 1B), portions of the C-terminal tail were deleted (Figure 1A; Δ74-133, Δ109-133, and Δ116-133 mutants), and the resulting truncation mutants were expressed in a *sna3*Δ strain. Whole cell lysates made from each strain were then analyzed by immunoblotting with an antibody to GFP to determine protein expression and vacuolar targeting. As expected, GFP-Sna3p^{WT} was detected as both the full-length fusion protein and free GFP (asterisk) in *sna3*Δ lysates (Figure 1C), consistent with previous reports of the localization and cleavage of the protein within the vacuole lumen (Reggiori and Pelham, 2001). In contrast, little to no free GFP was detected in lysates from cells expressing the C-terminal truncation mutants GFP-Sna3p$^{\Delta 116\text{-}133}$, GFP-Sna3p$^{\Delta 109\text{-}133}$, or GFP-Sna3p$^{\Delta 74\text{-}133}$ (Figure 1C), indicating either a disruption in vacuole delivery or diminished vacuolar protease activity in these cells.

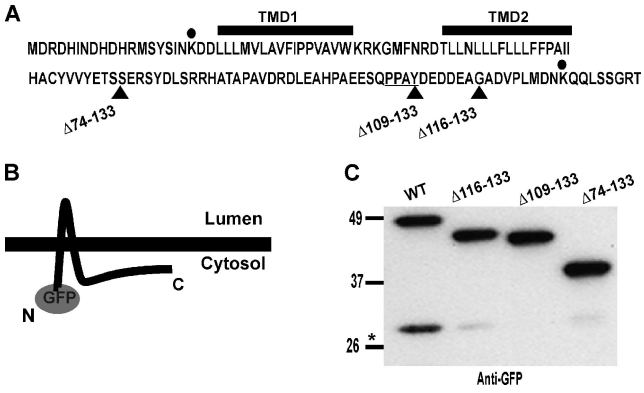

Figure 1. The C-terminal tail of Sna3p contains information for vacuolar sorting. (A) Sequence of Sna3p indicating transmembrane domains (TMD1 and TMD2), cytosolic lysine residues (black dots), and PPAY motif (underlined). Stop codons were introduced at the sites indicated by arrowheads, resulting in the deletion of residues 116-133, 109-133, and 74-133. (B) Schematic representation of the membrane topology of GFP-Sna3p^{WT}. (C) Immunoblot analysis using a mAb to GFP of whole cell lysates prepared from *sna3*Δ cells expressing full-length GFP-Sna3p^{WT}, GFP-Sna3p$^{\Delta 116\text{-}133}$, GFP-Sna3p$^{\Delta 109\text{-}133}$, and GFP-Sna3p$^{\Delta 74\text{-}133}$. The asterisk indicates the position of cleaved, free GFP. Numbers on the left indicate the positions of molecular mass markers (in kilodaltons).

To assess further the nature of this defect, the aforementioned strains were grown to mid-log phase at 30°C, labeled by uptake of the lipophilic dye FM4-64 to visualize the vacuolar membrane, and observed by fluorescence microscopy. Consistent with the immunoblotting results, *sna3*Δ cells expressing GFP-Sna3p^{WT} exhibited GFP fluorescence exclusively in the vacuole lumen (Figure 2, A–C). In contrast, GFP-Sna3p$^{\Delta 116\text{-}133}$ accumulated in several small cytoplasmic structures (an occasionally a larger structure), with little fluorescence in the vacuole (Figure 2, D–F). Interestingly, both GFP-Sna3p$^{\Delta 109\text{-}133}$ (Figure 2, G–I) and GFP-Sna3p$^{\Delta 74\text{-}133}$ (Figure 2, J–L) were also excluded from the vacuole; instead, they accumulated in a single, brightly fluorescing cytoplasmic structure. These structures seemed perivacuolar, and they were observed to partially overlap with the endocytic dye FM4-64 at discrete points within some cells. This indicated that at least some of these structures were endosomes.

These data confirmed that the decrease in free GFP observed in cell lysates of the aforementioned *sna3* C-terminal truncation mutants (Figure 1C) was due to a disruption in vacuolar delivery of Sna3p and not to decreased protease activity in the vacuole. Given the phenotypic similarities observed between GFP-Sna3p$^{\Delta 109\text{-}133}$ and GFP-Sna3p$^{\Delta 74\text{-}133}$

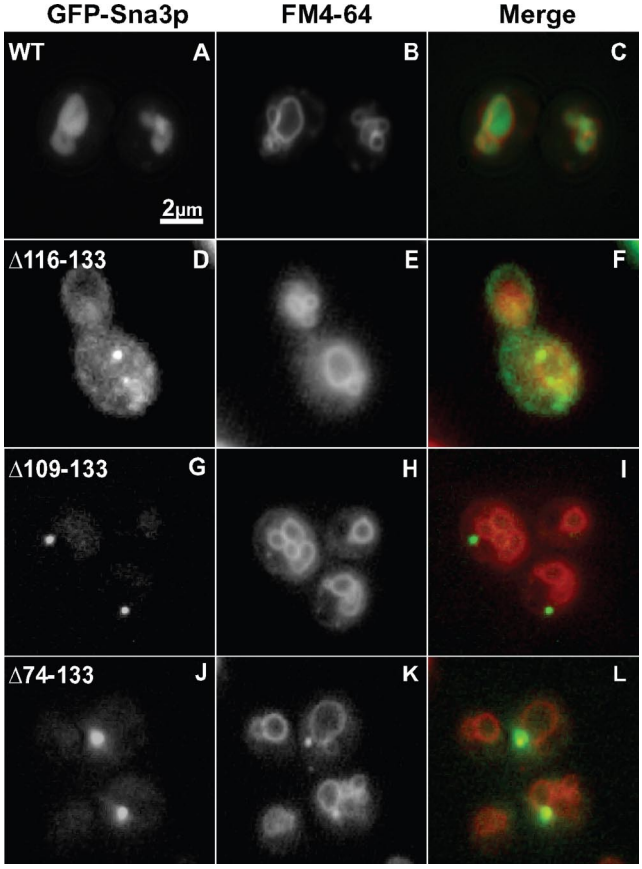

Figure 2. C-terminally truncated GFP-Sna3p accumulates in aberrant cytoplasmic structures that partially overlap with FM4-64. Wild-type (BY4742) strains expressing GFP-Sna3p^{WT} or the GFP-Sna3p C-terminal truncation mutants indicated in the figure were labeled in YPD with the endocytic tracer dye FM4-64 for 20 min, followed by a 30-min chase with fresh medium, and then they were examined by fluorescence microscopy.

mutants as well as the seemingly intermediate phenotype observed for GFP-Sna3p$^{\Delta 116\text{-}133}$, we concluded that a C-terminal portion of Sna3p spanning amino acid residues 109-133 (Figure 1A) is essential for its vacuolar sorting.

C-Terminally Truncated Sna3p Accumulates in an Aberrant Structure That Only Partially Overlaps with the Class E Compartment

Because similar results were obtained from deleting residues 109-133 or 74-133, further characterization of GFP-Sna3p trafficking focused on cells expressing GFP-Sna3p$^{\Delta 109\text{-}133}$. Previous studies have characterized Sna3p as a biosynthetic cargo molecule that undergoes ESCRT-dependent sorting into MVBs (Reggiori and Pelham, 2001). As with many other biosynthetic cargoes, vacuolar targeting of Sna3p is completely disrupted in class E Vps mutants, where it accumulates in aberrant MVBs. To determine whether the large punctate structures containing GFP-Sna3p$^{\Delta 109\text{-}133}$ were in fact aberrant MVBs, class E mutant (*vps27*Δ) cells expressing GFP-Sna3p^{WT} or GFP-Sna3p$^{\Delta 109\text{-}133}$ were labeled with FM4-64 and examined by fluorescence microscopy. As expected (Reggiori and Pelham, 2001), colocalization was observed between GFP-Sna3p^{WT} and FM4-64–labeled class E compartments in *vps27*Δ cells (Figure 3, A–C), confirming that Sna3p follows the MVB pathway to the vacuole. Strikingly, there seemed to be only partial overlap of the GFP-Sna3p$^{\Delta 109\text{-}133}$–containing structures with FM4-64–labeled class E structures (Figure 3, D–F). Thus, a fraction of the GFP-Sna3p$^{\Delta 109\text{-}133}$ seems to accumulate in a compartment that is distinct from the MVB.

We also examined the localization pattern of GFP-Sna3p^{WT} and GFP-Sna3p$^{\Delta 109\text{-}133}$ in *end3*Δ mutants, which are defective for endocytosis (Benedetti *et al*., 1994). In these cells, GFP-Sna3p^{WT} labeled the vacuole lumen (Figure 3G), confirming that Sna3p follows the biosynthetic pathway to the vacuole (Reggiori and Pelham, 2001). Interestingly, a pool of GFP-Sna3p$^{\Delta 109\text{-}133}$ was observed at the plasma membrane in *end3*Δ cells; however, most of the staining localized to the large cytoplasmic structures (Figure 3H). From these

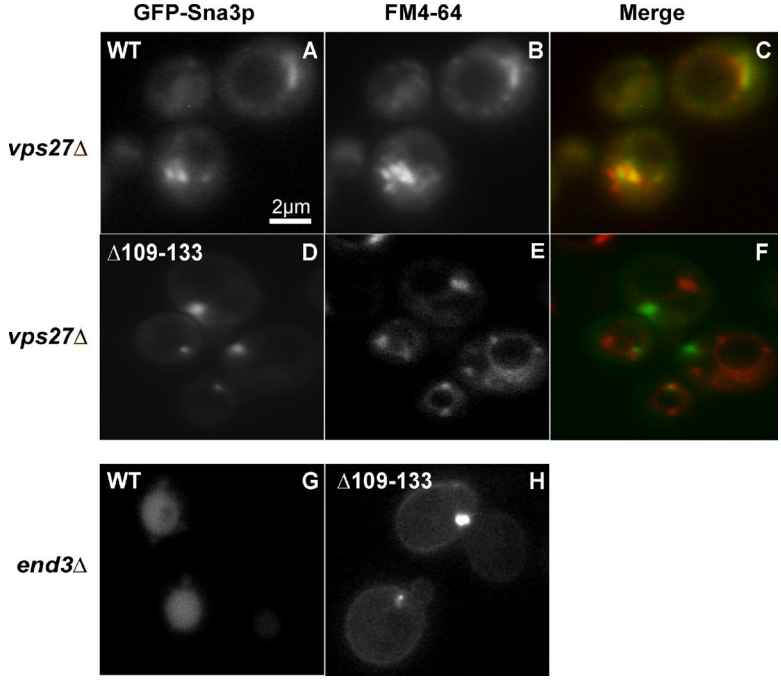

Figure 3. Structures containing C-terminally truncated GFP-Sna3p$^{\Delta 109\text{-}133}$ are mostly excluded from the MVB and transported through the biosynthetic pathway. Mutant *vps27*Δ cells expressing GFP-Sna3p^{WT} or GFP-Sna3p$^{\Delta 109\text{-}133}$ were labeled in YPD with the endocytic tracer dye FM4-64, for 20 min, followed by a 30-min chase with fresh medium, and then they were examined by fluorescence microscopy. (G–H) Fluorescence microscopy of *end3*Δ cells expressing GFP-Sna3p^{WT} or GFP-Sna3p$^{\Delta 109\text{-}133}$.

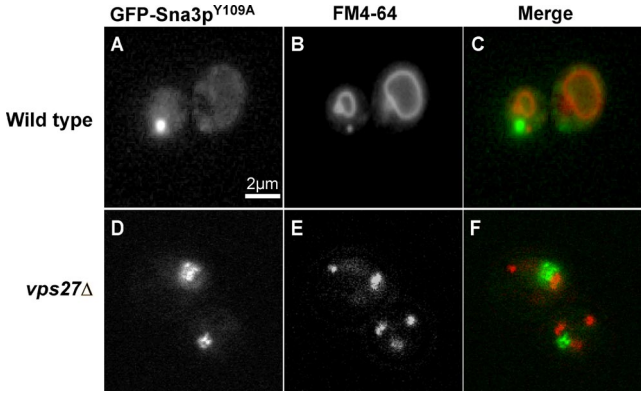

Figure 4. Y109A mutation is sufficient to disrupt Sna3p vacuolar targeting. Wild-type (BY4742) and *vps27*Δ strains expressing GFP-Sna3p^{Y109A} were labeled in YPD with the endocytic tracer dye FM4-64, for 20 min, followed by a 30-min chase with fresh medium, and then they were examined by fluorescence microscopy.

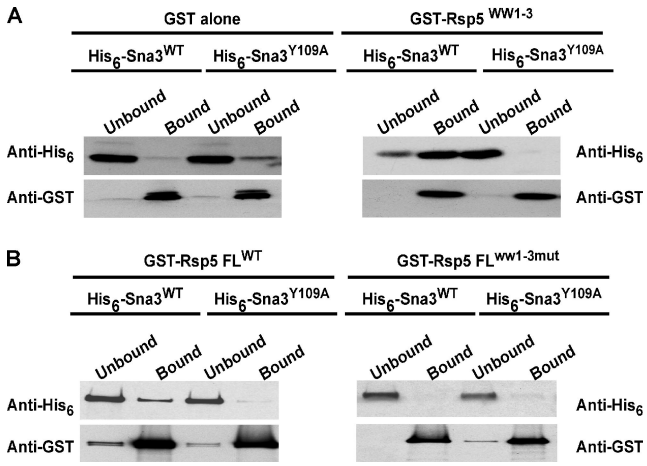

Figure 5. A PPAY motif in the C-terminal tail of Sna3p mediates binding to the WW domains of Rsp5p. (A) GST alone (26 kDa) and GST fused to all three WW domains of Rsp5p (GST-Rsp5^{WW1-3}; ~50 kDa) were bound to glutathione-agarose beads and incubated with *E. coli* lysates expressing His$_6$ fusions to the C-terminal tail of Sna3p, His$_6$-Sna3^{WT}, and His$_6$-Sna3^{Y109A} (~7 kDa). (B) GST fused to full-length Rsp5p (GST-Rsp5 FL^{WT}) and GST fused to full-length Rsp5p bearing mutations (W257A, W359A, and W415A) within its three WW domains (GST-Rsp5 FL$^{WW1-3\ mut}$) were bound to glutathione-agarose and incubated with *E. coli* lysates expressing His$_6$ fusions to the C-terminal tail of Sna3p, His$_6$-Sna3^{WT}, and His$_6$-Sna3^{Y109A} (~7 kDa). Bound proteins were analyzed by SDS-PAGE and immunoblotting with antibodies to His$_6$ and GST.

data, we concluded that the majority of GFP-Sna3p$^{\Delta 109\text{-}133}$ follows an intracellular pathway toward its aberrant compartment, although a small fraction may be diverted to the plasma membrane.

A PPXY Motif within the C-terminal Tail of Sna3p Is Required for Vacuolar Sorting and Mediates Binding to the WW Domains of Rsp5p

Having shown that the segment comprising amino acids 109-133 is important for Sna3p sorting to the vacuole, we next sought to identify the specific residues that may serve as a sorting signal. This region of Sna3p contains several interesting residues, including a Lys residue at position 125 (Figure 1A), which is deleted in the Δ109-133 mutant. Indeed, ubiquitinated Sna3p has been reported (Peng *et al*., 2003); however, studies by Reggiori and Pelham (2001) and our unpublished data have shown that mutation of both cytoplasmic Lys residues (K19 and K125) in GFP-Sna3p does not affect its vacuolar sorting. This rules out ubiquitination of Sna3p as a significant determinant of its sorting to the vacuole. Notably, also contained within residues 109-133 is the sequence PPAY (Figure 1A), which fits the PPXY motif common to ligands for WW domain-containing proteins such as the E3 ubiquitin ligase, Rsp5p (Sudol, 1996; Harty *et al*., 2000). The GFP-Sna3p$^{\Delta 109\text{-}133}$ mutant, which exhibits a similar localization pattern as the GFP-Sna3p$^{\Delta 74\text{-}133}$ mutant (Figure 2, G–L), consists of a conversion of Y109 within the PPAY sequence to a stop codon, resulting in the disruption of the PPXY motif.

To determine whether missorting of Sna3p was due to disruption of the PPAY motif, a single Y109A substitution was introduced within the C-terminal tail of wild-type GFP-Sna3p, and the mutant protein was expressed in *sna3*Δ cells. We observed that the Y109A mutation alone was sufficient to disrupt vacuolar targeting of GFP-Sna3p, resulting in a similar phenotype (i.e., accumulation in an aberrant cytoplasmic structure) to that of GFP-Sna3p$^{\Delta 109\text{-}133}$ in both wild-type (Figure 4, A–C) and *vps27*Δ cells (Figure 4, D–F).

Because PPXY motifs are ligands for WW domain-containing proteins (Sudol *et al*., 1995), and the WW domain-containing ubiquitin ligase Rsp5p has been implicated in MVB sorting (Katzmann *et al*., 2004; Morvan *et al*., 2004), we next sought to determine whether Sna3p can bind the WW domains of Rsp5p. To this end, His$_6$ fusions to C-terminal portions (amino acids 74-133) of wild-type (His$_6$-Sna3p^{WT}) and Y109A-mutant Sna3p (His$_6$-Sna3p^{Y109A}) were generated and expressed in *Escherichia coli*. Lysates were then incubated with glutathione-agarose beads loaded with purified GST or GST fused to all three WW domains of Rsp5 (GST-Rsp5p^{WW1-3}). We found that His$_6$-Sna3p^{WT} was able to bind GST-Rsp5p^{WW1-3} (Figure 5A, right) but not GST alone (Figure 5A, left). His$_6$-Sna3p^{Y109A}, in contrast, was unable to bind either GST or GST-Rsp5p^{WW1-3} (Figure 5A, left and right). To determine whether the WW domains are the sole determinants for this interaction, His$_6$-Sna3p^{WT} and His$_6$-Sna3p^{Y109A} lysates were also incubated with either GST fused to full-length Rsp5p (GST-Rsp5 FL^{WT}) or GST fused to full-length Rsp5 containing mutations (W257A, W359A, and W415A) within its three WW domains (GST-Rsp5 FL$^{WW1-3\ mut}$). As shown in Figure 5B, His$_6$-Sna3p^{WT} bound GST-Rsp5 FL^{WT} (left) but not GST-Rsp5 FL$^{WW1-3\ mut}$ (right), whereas the His$_6$-Sna3p^{Y109A} bound neither GST fusion (Figure 5B, left and right). Thus, the C-terminal tail of Sna3p binds Rsp5p through a PPXY-motif–WW domain interaction, and the WW domains of Rsp5p are both necessary and sufficient for binding.

Distinct Requirements for Rsp5p-mediated Sorting of Sna3p and Cps1p

Given the physical interaction of Sna3p with Rsp5p, we sought to determine whether mutations within the WW domains of Rsp5p had any effect on the vacuolar sorting of Sna3p. To this end, *rsp5*Δ cells expressing HA-Rsp5p^{WT} (*RSP5*) or HA-tagged Rsp5p consisting of WW domain mutations W257A, W359A, and W415A (*rsp5^{WW1-3}*) were transformed with GFP-Sna3p^{WT} and GFP-Cps1p (as a control). As reported previously (Katzmann *et al*., 2004; Morvan *et al*., 2004), GFP-Cps1p accumulated in a prevacuolar compartment as well as on the limiting membrane of the vacuole in *rps5^{WW1-3}* cells (Figure 6C). GFP-Sna3p^{WT} sorting was also

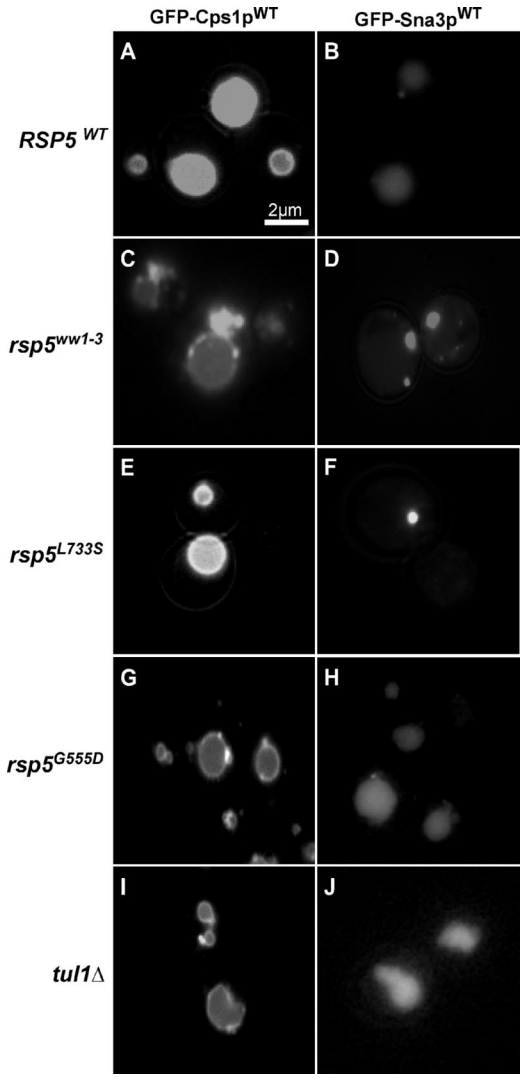

Figure 6. Sna3p and Cps1p display distinct requirements for Rsp5p activity. Fluorescence microscopy images comparing the localization patterns of GFP-Sna3p and GFP-Cps1p in *rsp5*Δ cells expressing HA-Rsp5p^{WT}, HA-Rsp5^{WW1-3}, HA-Rsp5p^{L733S}, HA-Rsp5p^{G555D}, and in *tul1*Δ cells.

affected in these mutants, but accumulated in usually 1 or 2 large cytoplasmic structures (Figure 6D) that were similar to those containing GFP-Sna3p^{Y109A} in *sna3*Δ cells (Figure 4, A–C). Thus, mutating the WW domains of Rsp5p seems to have distinct effects on the vacuolar sorting of GFP-Cps1p and GFP-Sna3p^{WT}.

Mutations within the catalytic HECT domain are another way to disrupt Rsp5p-mediated membrane trafficking events. Several catalytically defective *rsp5* alleles have been characterized thus far, including *rsp5-1* (herein referred to as *rsp5*^{L733S}), which contains a Leu-to-Ser substitution at residue 733. Leu-733 corresponds to hydrophobic residue (Leu or Phe) that is highly conserved among most HECT domains (Wang *et al*., 1999). This *rsp5* allele exhibits impaired ubiquitin–thioester formation and catalysis of substrate ubiquitination in vitro (Wang *et al*., 1999). Furthermore, *rsp5*^{L733S} displays endocytosis defects, and it is required for endocytic cargo ubiquitination and internalization (Gajewska *et al*., 2001; Dunn and Hicke, 2001a). Interestingly, this mutation was shown not to affect sorting of Cps1p (Katzmann *et al*., 2004). In contrast, another *rsp5* allele (*mvb326*), bearing a G555D mutation within the HECT domain (herein referred to as *rsp5*^{G555D}), was found to be defective for Cps1p ubiquitination but not for Ste2p ubiquitination at the permissive temperature (26°C) (Katzmann *et al*., 2004).

We sought to determine whether Sna3p sorting is affected by HECT domain mutations within Rsp5p by expressing GFP-Sna3p^{WT} and GFP-Cps1p in *rsp5*Δ cells expressing HA-Rsp5p^{WT}, HA-*rsp5p*^{L733S} or HA-*rsp5*^{G555D}. We observed that in both wild-type (Figure 6A) and *rsp5*^{L733S} cells (Figure 6E), GFP-Cps1p was detectable in the lumen of the vacuole, although some was also found on the limiting membrane of the vacuole. As reported previously (Katzmann *et al*., 2004), GFP-Cps1p sorting seemed significantly affected by the G555D mutation in Rsp5p, accumulating at perivacuolar structures and on the limiting membrane of the vacuole (Figure 6G). The differences between the Rsp5p L733S and G555D mutations on Cps1p sorting were more striking when endogenous Cps1p was analyzed by pulse-chase analysis in the aforementioned strains (Figure 7A). At 40 min of chase, no defect in Cps1p maturation was detected in wild-type or *rsp5*^{L733S} cells; however, a significant amount of precursor Cps1p remained in both *rsp5*$^{WW1-3}$ or *rsp5*^{G555D} cells (Figure 7A). Interestingly, the effects of *rsp5*^{L733S} and *rsp5*^{G555D} on GFP-Sna3p^{WT} vacuolar targeting were distinct from that of Cps1p. GFP-Sna3p^{WT} vacuolar delivery was completely disrupted in *rsp5*^{L733S} cells (Figure 6F), which exhibited a similar defect as the GFP-Sna3p$^{\Delta 109\text{-}133}$, GFP-Sna3p^{Y109A}, and *rsp5*$^{WW1-3}$ mutants, but it was unaffected in *rsp5*^{G555D} cells (Figure 6H). These results were confirmed by a biochemical assay to detect levels of cleaved GFP in *rsp5* mutants expressing GFP-Sna3p^{WT}. Cells were treated with cycloheximide to arrest protein synthesis for 60 min, and lysates were generated and analyzed by immunoblotting with an antibody to GFP. We observed that the majority of GFP-Sna3p^{WT} was detected as free GFP in wild-type and *rsp5*^{G555D} cells, consistent with their transport to the vacuole (Figure 7B). However, GFP-Sna3p^{WT} remained mostly uncleaved in *rsp5*$^{WW1-3}$ and *rsp5*^{L733S} extracts (Figure 7B). Together, these data indicate that both the WW domains and the HECT domain of Rsp5p are important for Sna3p sorting to the vacuole. Furthermore, our data demonstrate that, while both Cps1p and Sna3p depend on Rsp5p for vacuolar targeting, each has a distinct requirement for the ubiquitin ligase.

Given that Sna3p sorting is affected in *rsp5*$^{WW1-3}$ and *rsp5*^{L733S} cells, but not in *rsp5*^{G555D} cells, we sought to compare the effects of the L733S and G555D mutations on the Rsp5p–Sna3p interaction. A coimmunoprecipitation experiment was performed in *rsp5*Δ cells coexpressing HA-Rsp5p^{WT,} HA-Rsp5p$^{WW1\text{-}3\ mut}$, HA-*rsp5p*^{G555D}, or HA-*rsp5p*^{L733S} and GFP-Sna3p^{WT}. As expected, coimmunoprecipitation was observed between HA-Rsp5p^{WT} and GFP-Sna3p^{WT} (Figure 7C). Interestingly, although little effect on this interaction was detected with HA-*rsp5p*^{G555D,} a marked decrease in immunoprecipitated GFP-Sna3p^{WT} was observed with both HA-Rsp5p$^{WW1\text{-}3\ mut}$ and HA-*rsp5p*^{L733S}. These data indicate that residue L733S but not G555D is somehow important for the interaction between Rsp5p and Sna3p and that it may explain the differences in Sna3p sorting observed between *rsp5*^{G555D} and *rsp5*^{L733S} cells.

Tul1p is a RING family E3 ubiquitin ligase that has also been implicated in ubiquitin-dependent MVB sorting of some cargoes, including Cps1p (Reggiori and Pelham, 2002). To determine whether Sna3p sorting is Tul1p dependent, GFP-Cps1p and GFP-Sna3p^{WT} were expressed in *tul1*Δ cells (BY4742 background). As shown in Figure 6 (I and J), no

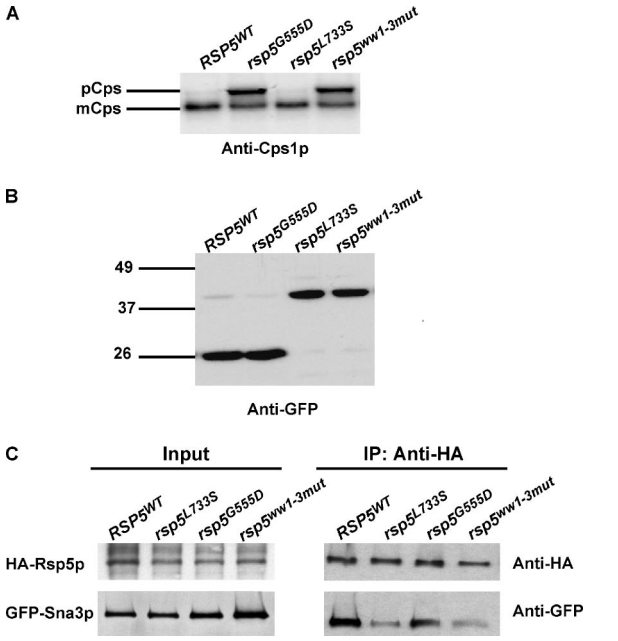

Figure 7. Biochemical assessment of Cps1p and Sna3p trafficking in *rsp5* mutants. (A) Mutant *rsp5*Δ strains expressing HA-Rsp5p^{WT}, HA-Rsp5p^{G555D}, HA-Rsp5p^{L733S}, or HA-Rsp5p$^{WW1\text{-}3mut}$ were labeled with [^{35}S]methionine for 10 min at 30°C and then chased in the presence of unlabeled methionine for 40 min. Endogenous Cps1p was immunoprecipitated from radiolabeled cell lysates and analyzed by SDS-PAGE and autoradiography. The positions of precursor Cps1p (pCps1p; ~73 kDa) and mature Cps1p (mCps1p; ~69 kDa) are indicated. (B) Mutant *rsp5*Δ strains coexpressing HA-Rsp5p^{WT}, HA-Rsp5p^{G555D}, HA-Rsp5p^{L733S}, or HA-Rsp5p$^{WW1\text{-}3mut}$ with GFP-Sna3p^{WT} were treated with cycloheximide to arrest protein synthesis for 60 min, and lysates were analyzed by SDS-PAGE and immunoblotting with an antibody to GFP. The positions of molecular mass markers (in kilodaltons) are indicated on the left. (C) Binding of GFP-Sna3p^{WT} to different Rsp5p HECT domain mutants. Coimmunoprecipitation experiments were performed in *rsp5*Δ cells coexpressing HA-Rsp5p^{WT}, HA-Rsp5p^{G555D}, HA-Rsp5p^{L733S}, or HA-Rsp5p$^{WW1\text{-}3mut}$ and GFP-Sna3p^{WT}. Cleared lysates were incubated for 2–4 h at 4°C with protein A-Sepharose beads bound to rabbit polyclonal antibody to the HA epitope, and immunoprecipitates were analyzed by immunoblotting with either mouse monoclonal anti-HA or mouse monoclonal anti-GFP antibodies.

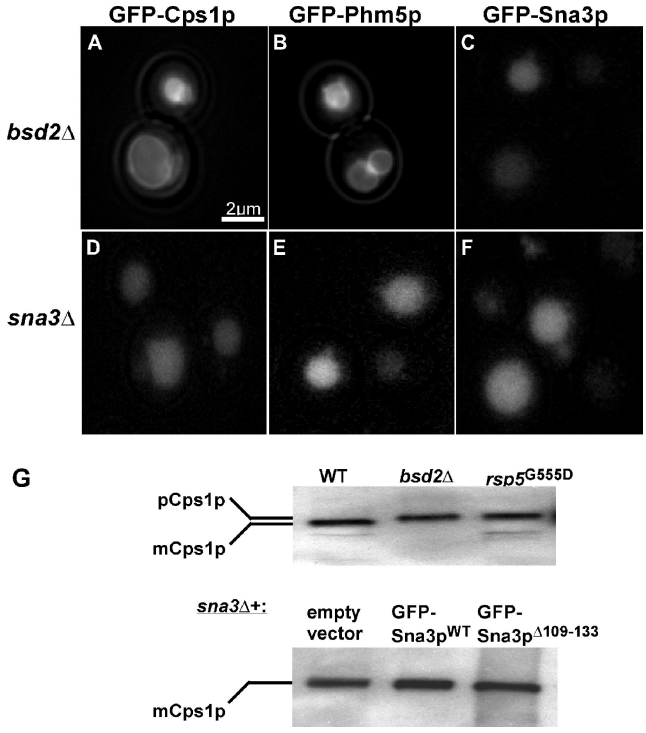

Figure 8. Sna3p sorts independently of Bsd2p. (A–F) Fluorescence microscopy images comparing the localization patterns of GFP-Cps1p, GFP-Phm5p, and GFP-Sna3p in *bsd2*Δ and *sna3*Δ cells. (G, top) Wild-type, *bsd2*Δ, and *rsp5*^{G555D} cells were labeled with [^{35}S]methionine for 10 min at 30°C and chased in the presence of unlabeled methionine for 40 min. Endogenous Cps1p was immunoprecipitated from radiolabeled cell lysates and analyzed by SDS-PAGE and autoradiography. (G, bottom) The same pulse chase assay described above was performed in *sna3*Δ cells expressing empty vector, GFP-Sna3p^{WT}, and GFP-Sna3p$^{\Delta 109\text{-}133}$. The positions of precursor Cps1p (pCps1p; ~73 kDa) and mature Cps1p (mCps1p; ~69 kDa) are indicated.

effect on the vacuolar targeting of Sna3p was observed in these cells, in contrast to Cps1p.

Sna3p Does Not Depend on Bsd2p for Vacuolar Targeting

Recent studies by Hettema *et al*. (2004) have identified the transmembrane protein Bsd2p as an adaptor for linking Rsp5p to some substrates. Bsd2p has a PPTY motif that binds to the WW domains of Rsp5p, and this interaction is important for sorting of various MVB cargoes. We sought to determine whether this interaction is also important for Sna3p MVB sorting by expressing GFP-Sna3p^{WT} in *bsd2*Δ cells. As shown in Figure 8 (A–C), although both GFP-Cps1p and GFP-Phm5p accumulated in the limiting membrane of the vacuole in *bsd2*Δ cells, there was no effect on GFP-Sna3p vacuolar targeting. Thus, GFP-Sna3p does not require Bsd2p for its MVB/vacuolar targeting, probably because it has its own PPXY motif.

Given that both Bsd2p and Sna3p are transmembrane proteins with cytosolic PPXY motifs that bind Rsp5p and that a Bsd2p–Rsp5p interaction mediates MVB sorting (Hettema *et al*., 2004), we wondered whether Sna3p may play a role in protein sorting. We therefore looked at MVB cargo sorting in *sna3*Δ cells. Compared with *bsd2*Δ, no defect in GFP-Cps1p or GFP-Phm5p vacuolar sorting was detected in *sna3*Δ cells (Figure 8, D–F). We also failed to detect an effect on endogenous Cps1p maturation in *sna3*Δ cells expressing empty vector, GFP-Sna3p^{WT}, or GFP-Sna3p$^{\Delta 109\text{-}133}$, compared with *bsd2*Δ or *rsp5*^{G555D} mutants (Figure 8G). Although these data do not exclude the possibility that Sna3p sorts other cargoes that do not rely upon Bsd2p for sorting, it seems that Sna3p behaves more like a cargo with an intrinsic ability to recruit Rsp5p.

DISCUSSION

Sna3p is a transmembrane protein that localizes to the lumen of the vacuole and undergoes ESCRT-dependent MVB sorting. Previous studies by Reggiori *et al*. (2001) clearly showed that, unlike other MVB cargoes, Sna3p does not require its direct ubiquitination for MVB sorting. However, the results presented in this article indicate that Sna3p MVB sorting is not entirely ubiquitin-independent in that, although its own ubiquitination is not necessary, a direct interaction with an ubiquitin ligase Rsp5p is crucial. We have identified a PPAY sequence within the C-terminal tail

of Sna3p that binds the WW domains of Rsp5p, and we showed that a single Y109A mutation within this sequence is sufficient to disrupt its MVB sorting. Consistent with these observations, we found that Sna3p is mislocalized in *rsp5* WW domain mutants.

Our results also indicate that mutations within the cytosolic C-terminal tail cause Sna3p to accumulate in an aberrant compartment that only partially overlaps with the class E compartment. Previous studies have shown that mutating ubiquitination target residues within other MVB cargo does not prohibit their delivery to late endosomes but rather their sorting into the intraluminal vesicles of MVBs. This causes their accumulation on the limiting membrane of the vacuole, rather than within the vacuolar lumen. Yet, we find that much of the Sna3p C-terminal mutants do not reach the class E compartment, much less the vacuole. Thus, the cytoplasmic structures accumulating mutant Sna3p may correspond to some endosomal or late Golgi intermediate along a pathway to the MVB. Exit of Sna3p from this compartment seems to require both the WW domains and the ubiquitinating activity of Rsp5p, although not the ubiquitination of Sna3p itself. It is currently unclear whether this compartment is shared by other MVB cargoes such as Cps1p or whether Sna3p and Cps1p transit via different intermediates. The latter possibility is plausible, given the findings by Bilodeau *et al*. (2002) that the ubiquitin binding activities of the ESCRT complex associated proteins Vps27p and Hse1p are not required for the MVB sorting of Sna3p.

We also report that Sna3p exhibits distinct requirements to those of Cps1p for sorting. Unlike Cps1p, Sna3p does not require either Bsd2p or Tul1p for vacuolar targeting. Furthermore, and perhaps most strikingly, Sna3p and Cps1p display distinct requirements for Rsp5p HECT domain ligase activity. Contrary to Cps1p, Sna3p is mislocalized in $rsp5^{L733S}$ (*rsp5-1*) but not $rsp5^{G555D}$ mutants. The finding that a specific HECT domain mutant of Rsp5p affects Sna3p sorting is puzzling, because direct ubiquitination of Sna3p is not required for its delivery to the vacuole (Reggiori and Pelham, 2001; our unpublished data). Also, because mutating the WW domains within GST-Rsp5 (full length) is sufficient to disrupt binding to His_6-Sna3p, the HECT domain does not seem to play a significant role in binding Sna3p.

One possibility is that there is an additional phenotype of the $rsp5^{L733S}$ mutant, other than its defective catalytic activity, which affects Sna3p sorting. One interesting finding by Wang *et al*. (2001) is that the $rsp5^{L733S}$ allele is mislocalized; Katzmann *et al*. (2004), in contrast, found no effect of the G555D mutation on Rsp5p localization. Thus, it is possible that the $rsp5^{L733S}$ mutant is simply spatially or conformationally unavailable to interact with Sna3p. This would be consistent with our observation that HA-tagged $rsp5^{L733S}$ exhibits significantly reduced binding to GFP-$Sna3p^{WT}$, compared with $Rps5^{WT}$ and $rsp5^{G555D.}$ These findings indicate that the Rsp5p L733S mutation somehow precludes efficient interaction with Sna3p and may explain the mislocalization of Sna3p in $rsp5^{L733S}$ mutants.

Another possibility is that the Rsp5p-mediated ubiquitination of some other protein is required for Sna3p sorting. Quite intriguing is the connection between Sna3p and actin cytoskeleton-associated proteins. A genome-wide two-hybrid screen identified an interaction between Sna3p and two actin cytoskeleton-associated proteins, Bzz1p/Lsb7p and Sla1p (Tong *et al*., 2002). Of notable interest, both of these proteins contain Src homology 3 domains, which allow them to bind proline-rich motifs and compete with WW domains for ligand binding in vitro (Sudol, 1996; Bedford *et al*., 1997). Rsp5p has previously been shown to interact with and regulate components of the actin cytoskeleton, including Sla1p (Kaminka *et al*., 2002; Stamenova *et al*., 2004). We now have evidence that Sna3p vacuolar sorting is disrupted in *sla1*Δ cells (our unpublished data). Thus, it is possible that Rsp5p HECT domain-mediated regulation of actin cytoskeletal or other sorting machinery components is important for the endosomal sorting of Sna3p. The mechanism for such a sorting pathway remains to be determined.

Although there can be no doubt that the Rsp5p–Sna3p interaction via the PPAY motif within residues 106–109 of Sna3p plays an essential role in Sna3p endosomal/vacuolar sorting, we cannot discount the possible existence of another sorting signal within residues C-terminal to the PPAY motif. Indeed, cells expressing GFP-$Sna3p^{\Delta 116\text{-}133}$ exhibit a significant vacuolar sorting defect in spite of having an intact PPAY motif. This suggests that there may be more than one sorting signal within the Sna3p C-terminal tail. This other signal must lie between residues 116 and 128, because a GFP-$Sna3p^{\Delta 128\text{-}133}$ mutant exhibits normal vacuolar targeting (our unpublished data). It is unlikely that the Δ116-133 mutation is affecting the Rsp5 interaction, because we do not see an effect on binding between GST-$Rsp5\ FL^{WT}$ and either GFP-$Sna3p^{\Delta 116\text{-}133}$ from yeast lysates, or purified His_6-$Sna3p^{\Delta 116\text{-}133}$ (our unpublished data). Further analysis of this region is required to identify the sorting determinant and function thereof.

During review of this manuscript, similar findings that Sna3p sorting is mediated by an interaction between its PPxY motif and the Rsp5p WW domains were reported by McNatt *et al*. (2006) and Oestreich *et al*. (2006). Both studies reported that ubiquitinated Sna3p can be detected under normal conditions, but they concluded that direct ubiquitination of Sna3p is not essential for its MVB sorting. Interestingly, Oestreich *et al*. (2006) did observe that ubiquitination of Sna3p enhances its sorting kinetics. This may at least partially explain our observed defect in the sorting of GFP-$Sna3p^{\Delta 116\text{-}133}$, because residue Lys125 is deleted in this mutant. Finally, although the Sna3p binding and ubiquitin–ligase activities of Rsp5p seem to be required for transport of Sna3p to late endosomes, it is possible that these activities may also mediate actual sorting of Sna3p into the intraluminal vesicles of MVBs upon arrival In this regard, Oestreich *et al*. (2006) reported some detection of GFP-tagged Sna3p on the limiting membrane of the vacuole in certain *rsp5* mutants

In conclusion, our findings demonstrate that the ubiquitination-independent sorting of a transmembrane cargo to the vacuole is nonetheless dependent on the binding and activity of an ubiquitin ligase. Therefore, ubiquitination enables sorting to the vacuole not just by tagging cargo but perhaps also by modifying the cargo sorting machinery.

ACKNOWLEDGMENTS

We thank Claudio Aguilar (Purdue University, Indiana), Linda Hicke, Teresa Zoladek, Kai Simons, Hugh Pelham, Greg Payne, and Scott Emr (UCSD, California) for strains and plasmids. We also thank Hsin-I Tsai for technical support and Cecilia Bonangelino and Haruki Hasegawa for plasmid construction.

REFERENCES

Babst, M. (2005). A protein's final ESCRT. Traffic *6*, 2–9.

Bedford, M. T., Chan, D. C., and Leder, P. (1997). FBP WW domains and the Abl SH3 domain bind to a specific class of proline-rich ligands. EMBO J. *16*, 2376–2383.

Benedetti, H., Raths, S., Crausaz, F., and Riezman, H. (1994). The END3 gene encodes a protein that is required for the internalization step of endocytosis and for actin cytoskeleton organization in yeast. Mol. Biol. Cell *5*, 1023–1037.

Bilodeau, P. S., Urbanowski, J. L., Winistrofer, S. C., and Piper, R. C. (2002). The Vps27p Hse1p complex binds ubiquitin and mediates endosomal protein sorting. Nat. Cell Biol. *4*, 534–539.

Bonangelino, C. J., Chavez, E. M., and Bonifacino, J. (2002). Genomic screen for vacuolar protein sorting genes in *Saccharomyces cerevisiae.* Mol. Biol. Cell *13*, 2486–2501.

Dunn, R., and Hicke, L. (2001a). Domains of the Rsp5 ubiquitin-protein ligase required for receptor-mediated and fluid-phase endocytosis. Mol. Biol. Cell *12*, 421–435.

Dunn, R., and Hicke, L. (2001b). Multiple roles for Rsp5p-dependent ubiquitination at the internalization step of endocytosis. J. Biol. Chem. *276*, 25974–25981.

Gajewska, B., Kaminka, J., Jesionowska, A., Martin, N. C., Hopper, A. K., and Zoladek, T. (2001). WW domains of Rsp5p define different functions: determination of roles in fluid phase and uracil permease endocytosis in *Saccharomyces cerevisiae*. Genetics *157*, 91–101.

Harty, R. N., Brown, M. E., Wang, G., Huibregtse, J., and Hayes, F. P. (2000). APPxY motif within the VP40 protein of Ebola virus interacts physically and functionally with a ubiquitin ligase: implications for filovirus budding. Proc. Natl. Acad. Sci. USA *97*, 13871–13876.

Hettema, E. H., Valdez-Taubas, J., and Pelham, H. R. (2004). Bsd2 binds the ubiquitin ligase Rsp5 and mediates the ubiquitination of transmembrane proteins. EMBO J. *23*, 1279–1288.

Hicke, L., and Dunn, R. (2003). Regulation of membrane protein transport by ubiquitin and ubiquitin-binding proteins. Annu. Rev. Cell Dev. Biol. *19*, 141–172.

Hurley, J., and Emr, S. D. (2006). The ESCRT complexes: structure and mechanism of a membrane-trafficking network. Annu. Rev. Biophys. Biomol. Struct. *35*, 277–289.

Kaminka, J., Gajewska, B., Hopper, A. K., and Zoladek, T. (2002). Rsp5p, a new link between the actin cytoskeleton and endocytosis in the yeast *Saccharomyces cerevisiae*. Mol. Cell. Biol. *22*, 6946–6948.

Katzmann, D. J., Babst, M., and Emr, S. D. (2001). Ubiquitin-dependent sorting into the multivesicular body pathway requires the function of a conserved endosomal protein sorting complex, ESCRT-I. Cell *106*, 145–155.

Katzmann, D. J., Odorizzi, G., and Emr, S. D. (2002). Receptor downregulation and multivesicular-body sorting. Nat. Rev. Mol. Cell Biol. *3*, 893–905.

Katzmann, D. J., Sarkar, S., Chu, T., Audhya, A., and Emr, S. D. (2004). Multivesicular body sorting: ubiquitin ligase Rsp5 is required for the modification and sorting of carboxypeptidase S. Mol. Biol. Cell *15*, 468–480.

McNatt, M. W., McKittrick, I., West, M., and Odorizzi, G. (2006). Direct binding to Rsp5 mediates ubiquitin-independent sorting of Sna3 via the multivesicular body pathway. Mol. Biol. Cell *18*, 697–706.

Morvan, J., Froissard, M., Haguenauer-Tsapis, R., and Urban-Grimal, D. (2004). The ubiquitin ligase Rsp5p is required for modification and sorting of membrane proteins into multivesicular bodies. Traffic *5*, 383–392.

Odorizzi, G., Babst, M., and Emr, S. D. (1998). Fab1p PtdIns(3)P 5-kinase function essential for protein sorting in the multivesicular body. Cell *95*, 847–858.

Oestreich, A. J., Aboian, M., Lee, J., Azmi, I., Payne, J., Issaka, R., Davies, B., and Katzmann, D. J. (2006) Characterization of multiple MVB sorting determinants within Sna3, a role for the rsp5 ubiquitin ligase. Mol. Biol. Cell *18*, 707–720.

Peng, J. Schwartz, D., Elias, J. E., Thoreen, C. C., Cheng, D., Marsischky, G. Roelofs, J., Finley, D., and Gygi, S. P. (2003). A proteomics approach to understanding protein ubiquitination. Nat. Biotechnol. 8, 921–926.

Reggiori, F., Black, M. W., and Pelham, H. R. (2000). Polar transmembrane domains target proteins to the interior of the yeast vacuole. Mol. Biol. Cell *11*, 3737–3749.

Reggiori, F., and Pelham, H. R. (2001). Sorting of proteins into multivesicular bodies: ubiquitin-dependent and -independent targeting. EMBO J. *20*, 5176–5186.

Reggiori, F., and Pelham, H. R. (2002). A transmembrane ubiquitin ligase required to sort membrane proteins into multivesicular bodies. Nat. Cell Biol. *4*, 117–123.

Rieder, S. E., Banta, L. M., Kohrer, K., McCaffery, J. M., and Emr, S. D. (1996). Multilamellar endosome-like compartment accumulates in the yeast vps28 vacuolar protein sorting mutant. Mol. Biol. Cell *7*, 985–999.

Stamenova, S. D., Dunn, R., Adler, A. S., and Hicke, L. (2004). The Rsp5 ubiquitin ligase binds to and ubiquitinates members of the yeast CIN85-endophilin complex, Sla1-Rvs167. J. Biol. Chem. *279*, 16017–16025.

Sudol, M. (1996). Structure and function of the WW domain. Prog. Biophys. Mol. Biol. *65*, 113–132.

Sudol, M., Chen, H. I., Bougeret, C., Eindbond, A., and Bork, P. (1995). Characterization of a novel protein-binding module—the WW domain. FEBS Lett. *369*, 67–71.

Tong, A. H. *et al*. (2002). A combined experimental and computational strategy to define protein interaction networks for peptide recognition modules. Science *295*, 321–324.

Urbanowski, J. L., and Piper, R. C. (2001). Ubiquitin sorts proteins into the intralumenal degradative compartment of the late-endosome/vacuole. Traffic *2*, 622–630.

Wang, G., Yang, J., and Huibregtse, J. M. (1999). Functional domains of the Rsp5 ubiquitin-protein ligase. Mol. Cell. Biol. *19*, 342–352.

Wang, G., McCaffery, J. M., Wendland, B., Dupre, S., Haguenauer-Tsapis, R., and Huibregtse, J. M. (2001). Localization of the Rsp5p ubiquitin-protein ligase at multiple sites within the endocytic pathway. Mol. Cell. Biol. *21*, 3564–3575.